

Spatially Coupled Repeat-Accumulate Coded Cooperation

Naoki Takeishi and Koji Ishibashi

Advanced Wireless Communication Research Center (AWCC)

The University of Electro-Communications, 1-5-1 Chofugaoka, Chofu-shi, Tokyo 182-8585, Japan

Email: takeishi@awcc.uec.ac.jp, koji@ieee.org

Abstract—In this paper, a new coded cooperation scheme called *spatially coupled repeat-accumulate coded cooperation* (SC-RA-CC) is proposed for multiple access channels (MAC) with a large number of users and one common destination. The proposed approach combines two advantages of repeat-accumulate (RA) codes and spatial coupling. RA codes show the superior decoding performance with the simple encoding and spatial coupling exhibits the so-called *threshold saturation* behavior; the threshold of coupled codes with sub-optimal belief propagation (BP) decoding asymptotically achieves the optimal maximum *a posteriori* (MAP) decoding threshold. Our SC-RA-CC can be considered as the distributed version of spatially coupled repeat-accumulate codes which provide the higher spatial diversity and coding gain when both the number of users and the size of packets are limited. The performance of the proposed coded cooperation is analyzed via density evolution (DE). Numerical results confirm that SC-RA-CC can efficiently obtain even higher diversity and coding gain than both direct transmission and conventional adaptive network coded cooperation (ANCC).

Index Terms—Wireless sensor networks (WSNs), repeat-accumulate codes, spatially coupled codes, coded cooperation, density evolution.

I. INTRODUCTION

Multiple access channels (MAC) with a large number of users and one common destination have been actively investigated to design many-to-one wireless communications systems such as wireless sensor networks (WSNs) for environmental monitoring, disaster prevention, and so on [1]. The information should be reliably and efficiently transmitted over the wireless channels while the channels are typically unreliable due to the multipath fading. When the channel coherence time is longer than a transmission frame, i.e., flat fading, and the signal power at the destination is deeply faded, the channel coding does not help anymore. The use of multiple antennas at the transmitter and/or receiver side can effectively mitigate the effect of fading even in flat fading channels [2, 3]. However, for many applications such as WSNs, the deployment of multiple antennas is too costly in terms of size and power consumption.

To this end, cooperative diversity protocols such as amplify-and-forward (AF) and decode-and-forward (DF) protocols have been proposed, which demonstrate a potential to achieve a diversity gain or enhance the capacity of wireless systems without deploying multiple antennas at every nodes [4]. Furthermore, *coded cooperation* has been proposed to obtain not only the spatial diversity gain but also the coding gain through the cooperation [5]. Due to the half duplex constraint, the

protocol of coded cooperation is composed of two steps; at the first step, all transmit nodes sequentially broadcast their information packets. At the second step, every node independently encodes a parity packet based on the others' packets correctly decoded at the first step and transmits it to the destination. At the destination, every information packet and corresponding parity packet composes a codeword where parity packets are transmitted over mutually independent wireless channels. Coded cooperation, hence, can enjoy both the spatial diversity gain and coding gain.

Adaptive network coded cooperation (ANCC) has been subsequently proposed for a large-scale network with a large number of transmit nodes [6]. The idea of ANCC is to dynamically map the subgraph of the network topology to the graph of codes by randomly XORing several packets out of the successfully received ones. The resulting codes form the low-density generator-matrix (LDGM) codes which is a special class of low-density parity-check (LDPC) codes [7]. Although the sufficiently long codeword length is necessary to enhance the decoding performance of LDGM codes [8], the codeword length of ANCC is given by the double of the number of transmit nodes, regardless of the size of information packets. Therefore, if the number of transmit nodes is limited, the decoding performance of ANCC would have a large gap from the theoretical limit of the underlying codes. Moreover, in order to decode these coded packets, the destination should have the knowledge of entire underlying graph. In practice, the overhead informing such information becomes considerably large which leads to the loss of bandwidth efficiency of the system. The question that may arise here is how to achieve the decoding performance approaching to the channel capacity with practical encoding and decoding complexity when both the number of users and the length of information packets are limited.

In this paper, we propose a new coded cooperation scheme named *spatially coupled repeat-accumulate coded cooperation* (SC-RA-CC). Repeat-accumulate (RA) codes have been proposed in [9] as turbo-like codes, which show the decoding performance comparable to turbo codes [10] while its encoding complexity is lower. More recently, spatially coupled LDPC code has been proposed in [11]. The remarkable invention of this code is *spatial coupling* that exhibits the so-called *threshold saturation* behavior; the threshold of coupled codes with sub-optimal BP decoding asymptotically achieves the

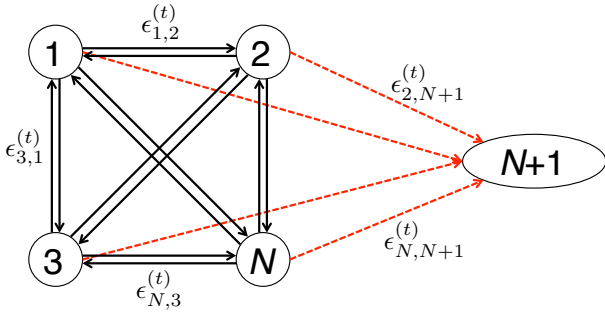


Fig. 1. System model of cooperative network consisting of N transmit nodes and a common destination.

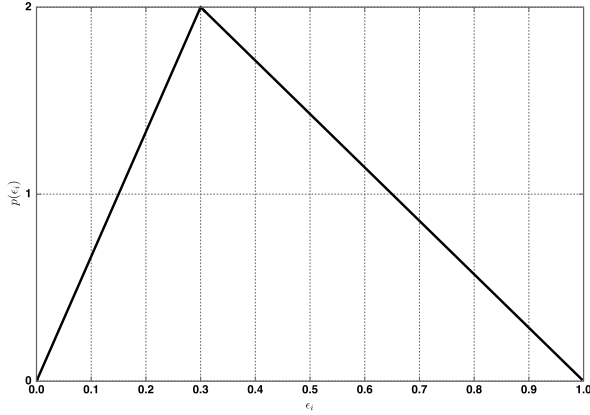


Fig. 2. Triangle distribution for evaluate spatial diversity.

optimal maximum *a posterior* (MAP) decoding threshold. Based on these seminal works, spatially coupled RA codes have been proposed to combine two advantages of RA codes and spatial coupling, namely low complexity encoding and significantly superior decoding performance [12]. SC-RA-CC can be considered as a distributed version of spatially coupled repeat-accumulate codes while the proposed approach still shows the superior decoding performance close to the channel capacity even when both the number of users and the length of information packets are limited.

This paper is organized as follows. In Section II, we briefly describe the system model assumed in this paper. The encoding protocol of proposed SC-RA-CC is described in Section III. In Section IV, the threshold of SC-RA-CC with BP decoding is theoretically analyzed by using the density evolution. In Section V, computer simulations are performed to confirm the analytical results and compare the performance of SC-RA-CC with the direct transmission and conventional ANCC. Finally, Section VI concludes this work.

II. SYSTEM MODEL

In this paper, we consider a network with N transmit nodes and a common destination as illustrated in Fig. 1. Each node is equipped with a single antenna and subject to the half-duplex constraint. Thus, we assume that while listening to the channel, the node may not transmit. Each node sequentially

transmits their own packets to the common destination based on the time division multiple access (TDMA). We here define a *transmission block* as a time period that N nodes transmit their own packets and assume that every node transmits T different packets through T transmission blocks.

In this paper, wireless channels are modeled as binary erasure channel (BEC). This model simplifies the mathematical analysis of error-correcting codes. Moreover, in order to model the effect of slow fading, we assume that the bit erasure probability does not change during T consecutive transmission blocks. In typical cooperative communications, the transmit nodes are closely-placed and thus the average received signal power at the transmit nodes is even higher than that at the destination. Therefore, we assume that the channels between the transmit nodes are ideally error-free for simplicity. Then, bit erasure probability from node $i \in \{1, 2, \dots, N\}$ to $j \in \{1, 2, \dots, N + 1\}$ at transmission block $t = 1, 2, \dots, T$ can be written as

$$\epsilon_{i,j}^{(t)} = \begin{cases} 0 & (1 \leq j \leq N) \\ \epsilon_i & (j = N + 1) \end{cases}. \quad (1)$$

Here $(N + 1)$ is a index of the destination node and ϵ_i denotes the bit erasure probability of the channel between node i to the destination node. Note that, in coded cooperation, $(T + 1)$ transmission blocks are needed to transmit T different information packets of every user, which will be explained in detail in the next section.

To evaluate the coding gain and diversity gain obtained by our proposed approach, we consider the following two different channel models.

1) *Constant Channel Model*: In this model, the erasure probability of every channel link between node i to the destination is given by a constant erasure probability $\bar{\epsilon}$, namely $\epsilon_i = \bar{\epsilon}$. This channel model is suitable to evaluate the pure coding gain obtained by the proposed approach.

2) *Triangle Distribution Channel Model*: As mentioned above, coded cooperation aims to exploit not only the coding gain but also the spatial diversity gain. To evaluate the potential of spatial diversity enhancement of proposed cooperation, the constant channel model is inadequate since the model does not have any difference between different channel links. Thus, we further introduce a *triangle distribution channel model* which can be considered as a simplified fading model. In this model, erasure probability is characterized by the triangle distribution of which probability density function (pdf) $f(x)$ is given by

$$f(x) = \begin{cases} \frac{2x}{3\bar{\epsilon}-1} & 0 \leq x \leq 3\bar{\epsilon} - 1 \\ \frac{2(x-1)}{3\bar{\epsilon}} & 3\bar{\epsilon} - 1 < x \leq 1 \end{cases}. \quad (2)$$

Note that the average erasure probability $\bar{\epsilon}$ in this model should be $\frac{1}{3} \leq \bar{\epsilon} \leq \frac{2}{3}$. Figure 2 illustrates the pdf with $\bar{\epsilon} = 1.3/3$ as an example.

III. SPATIALLY COUPLED REPEAT-ACCUMULATE CODED COOPERATION

In this section, the encoding of SC-RA-CC is explained. Moreover, two different graph expressions of SC-RA-CC are

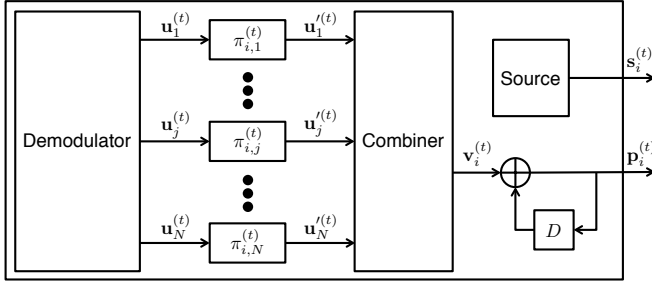


Fig. 3. Encoding block diagram of SC-RA-CC for the transmit node i at the t th transmission block.

given so as to elaborate the structure of SC-RA-CC achieving the superior performance.

A. Encoding

Encoding block diagram of transmit nodes i at the t th transmission block is illustrated in Fig. 3. Let $s_i^{(t)}$ denote K -bit information packet generated by transmit node i at the t th transmission block. A K -bit binary vector $\mathbf{u}_j^{(t)}$ indicates the latest information packet transmitted by node j at the t th transmission block and thus it can be rewritten by

$$\mathbf{u}_j^{(t)} = \begin{cases} \mathbf{s}_j^{(t)} & (j < i) \\ \mathbf{s}_j^{(t-1)} & (j > i) \end{cases}. \quad (3)$$

The vector $\mathbf{u}_j^{(t)}$ is interleaved by corresponding interleaver $\pi_{i,j}^{(t)}$ and the resulting binary vector is denoted by $\mathbf{u}_j'^{(t)}$. Note that the interleaver $\pi_{i,j}^{(t)}$ is mutually and stochastically independent of ones with different t , i , and j . As observed in the figure, every transmission block, the transmit node i has $(N-1)$ interleaved vectors. These $(N-1)$ vectors are combined into a K -bit vector $\mathbf{v}_i^{(t)}$ by the following equation:

$$\mathbf{v}_i^{(t)} = \bigoplus_{\substack{j=1 \\ j \neq i}}^N \mathbf{u}_j'^{(t)}, \quad (4)$$

where \bigoplus expresses bit-by-bit XOR operation. Finally, a K -bit parity packet $\mathbf{p}_i^{(t)}$ is obtained by differentially encoding the vector $\mathbf{v}_i^{(t)}$ as illustrated in Fig. 3. The node i transmits $\mathbf{s}_i^{(t)}$ and $\mathbf{p}_i^{(t)}$ as its own message to the destination at the t th transmission block.

Note that, at the first transmission block i.e., $t = 1$, first $(N-1)$ transmit nodes do not have $(N-1)$ information packets from the others to calculate (4). In this case, node j just encodes $(j-1)$ packets. Similarly, at the last transmission block i.e., $t = T+1$, transmit nodes do not have new information packets anymore but the transmit node j has $(N-j)$ packets to be encoded. Also note that the last user $j = N$ at the last transmission block $t = T+1$ does not have any packets to transmit. Therefore, the resulting coding rate of SC-RA-CC R is calculated as $R = \frac{TN}{2TN+N-2}$.

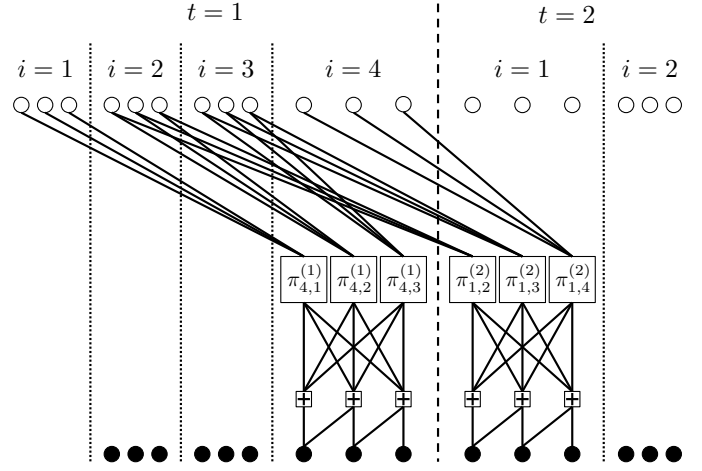


Fig. 4. Tanner-graph of SC-RA-CC with $K = 3$ and $N = 4$ where parity bits of user 4 at $t = 1$ and user 1 at $t = 2$ are only illustrated.

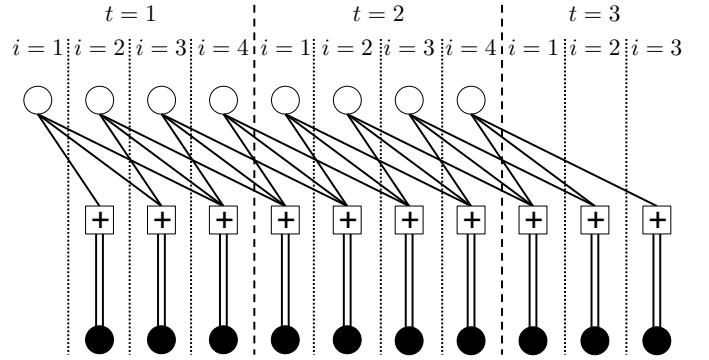


Fig. 5. Protograph of SC-RA-CC with $N = 4$ and $T = 2$.

B. Graph Expressions of SC-RA-CC

To clearly show the structure of SC-RA-CC, we here introduce a representation of bipartite graph called Tanner-graph. Figure 4 is a Tanner-graph of SC-RA-CC with $N = 4$ and $K = 3$ at the arbitrary transmission block t where circles indicate variable nodes corresponding to coded bits and squares indicate check nodes corresponding to a single parity check constraint. Also, white and black circles respectively indicate information and parity bits. Note that, in Fig. 4, parity bits of user 4 at $t = 1$ and user 1 at $t = 2$ are only illustrated for simplicity.

As explained above, every transmit node utilizes $(N-1)$ information packets to encode the parity packet. The parity of node 4 is obtained by XORing the interleaved information bits of three users. Subsequently, node 1 would combine three information packets with corresponding interleavers to encode the parity packet at the next transmission block.

To further elaborate the structure of SC-RA-CC, we introduce a protograph [13] of SC-RA-CC. Figure 5 shows the protograph with $N = 4$ and $T = 2$. The graph has white and black circles respectively indicating K -bit information packets and parity packets, i.e., variable nodes. Also, square nodes indicate check nodes. Note that the edges between

white variable nodes and check nodes include the operation of random permutation (cf., Fig 4). As obvious from the figure, check nodes are connected with spatially-close variable nodes and check nodes on both ends of the graph have less edges than those in the center. The corresponding variable nodes of check nodes with less edges would be successfully decoded with high probability and this phenomenon would be propagated to nodes in the center with the aid of BP decoder [14], which results in the superior performance of SC-RA-CC. Also, transmit node 1 at the first transmission block $t = 1$ does not have the parity packet and transmit node 4 at the last transmission block $t = 3$ do not have any packets to transmit as described in Section III-A.

This protograph representation clearly explains how the cooperation exploits the network structure to construct the code even when the number of users and the length of information packet are limited. Different from ANCC, spatially coupled parity packets of SC-RA-CC contribute the decoding of $N \times T$ information packets and thus SC-RA-CC can efficiently construct the long codeword enough.

It is also worth noting that the SC-RA-CC does not require the overhead to inform the XOR operation of every transmit node. Different from ANCC, every nodes always combine all the received packets without randomly choosing them.

IV. DENSITY EVOLUTION ANALYSIS

In this section, the decoding threshold of SC-RA-CC is analyzed by density evolution [15].

1) *Constant Channel*: Density evolution tracks average bit erasure probability of every packets upon BP decoding. As obvious from the protograph of SC-RA-CC described in Section III-B, variable nodes corresponding to information packets and parity packets have the different number of edges. Thus, we separately derive the bit erasure probability of these nodes.

Upon l iterations of BP decoding, bit erasure probability of information packet $x_{t,i}^{(l+1)}$ and parity packet $y_{t,i}^{(l+1)}$ are respectively calculated by

$$x_{t,i}^{(l+1)} = \epsilon_i \left(\frac{1}{N-1} \sum_{j=1}^{N-1} \left(1 - (1 - \mu(y, i+j))^2 \times \prod_{k=1, j \neq k}^{N-1} (1 - \mu(x, i+j-k)) \right) \right)^{N-2} \quad (5)$$

and

$$y_{t,i}^{(l+1)} = \epsilon_i \left(1 - (1 - \mu(y, i)) \times \prod_{k=1}^{N-1} (1 - \mu(x, i-k)) \right), \quad (6)$$

where the function $\mu(\alpha, \beta)$ calculates the index of α by

$$\mu(\alpha, \beta) = \begin{cases} \alpha_{t-1, \beta+N}^{(l)} & (\beta \leq 0) \\ \alpha_{t, \beta}^{(l)} & (0 < \beta \leq N) \\ \alpha_{t+1, \beta-N}^{(l)} & (N \leq \beta) \end{cases}. \quad (7)$$

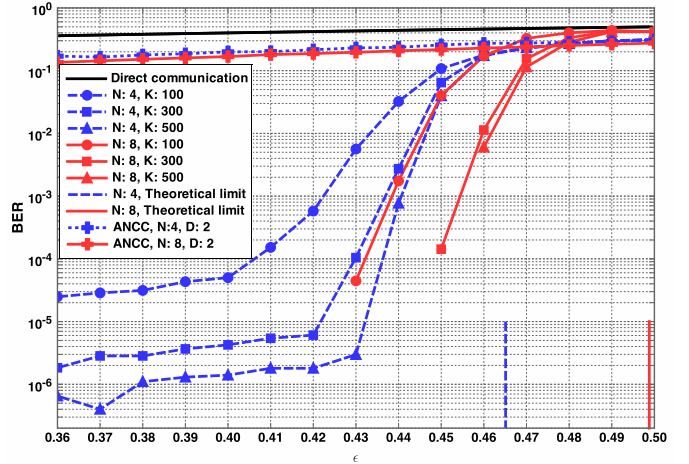


Fig. 6. BER versus bit erasure probability $\bar{\epsilon}$ graph on constant channel.

The decoding threshold of BP decoding ϵ^{th} is defined as

$$\epsilon^{\text{th}} \triangleq \sup \left\{ \epsilon > 0 \left| \lim_{l \rightarrow \infty} x_{\forall t, \forall i}^{(l)} = 0 \right. \right\} \quad (8)$$

For the erasure probability below this threshold, decoding erasure probability goes to zero. Finally, the bit erasure probability $\bar{\epsilon}$ is simply used instead of ϵ_i for the constant channel.

2) *Triangle Distribution Channel*: To evaluate the achievable diversity gain of cooperation, we evaluate the outage probability rather than ϵ^{th} averaged over the channel realization where the outage event occurs when the decoding erasure probability does not go to zero upon decoding. Thus outage probability can be defined as

$$P_o \triangleq \mathbb{E} \left[\Pr \left(\lim_{l \rightarrow \infty} x_{\forall t, \forall i}^{(l)} > 0 \right) \right]. \quad (9)$$

The outage probability of direct communication is simply calculated by

$$P_o = \mathbb{E} \left[\int_0^{\epsilon^{\text{th}}} f(x) dx \right], \quad (10)$$

where the function $f(x)$ is given by (2) and ϵ^{th} is calculated by (8). Also, the outage probability of SC-RA-CC is numerically calculated using (5) and (6).

V. NUMERICAL RESULTS

In this section we shows numerical results of computer simulation and density evolution analysis. In the following, we assume that $T = 20$ and the maximum number of iterations in every BP decoding is 300.

A. Constant Channel

Figure 6 shows the bit erasure rate (BER) of direct communication, SC-RA-CC, and conventional ANCC [6] where the length of information packets is assumed to be $K = 100, 300,$ and 500 and the number of transmit nodes is assumed to be $N = 4$ and 8 . For ANCC, the degree D is set to be 2 that is optimized via computer simulations. Theoretical limits

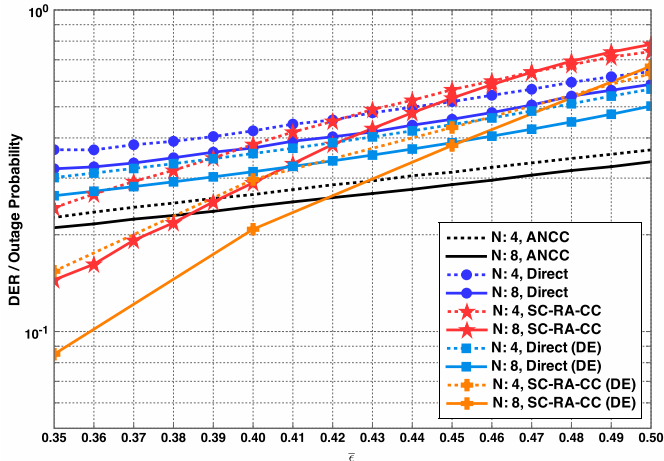


Fig. 7. DER versus average bit erasure probability $\bar{\epsilon}$ over triangle distributed channels.

of SC-RACC with $N = 4$ and 8 are also presented, which are calculated by (8). Note that the coding rate of SC-RACC with $N = 4$ and 8 and conventional ANCC is 0.494 , 0.491 , and 0.5 , respectively.

Comparing with the direct transmission and conventional ANCC, SC-RACC significantly improves the decoding performance because of high coding gain. Also, SC-RACC provides the lower BER as K increases since the codeword length of SC-RACC is proportional to both the length of information packets and the number of users while that of ANCC only depends on the number of users. However, gaps between simulation results and decoding thresholds obtained by density evolution are still observed, which are about 0.04 . This is because, in the calculation of density evolution, the infinite codeword length is assumed while the codeword length in simulations is limited.

The performance of $N = 4$ exhibits the error floor even when $K = 500$. SC-RACC couples $(N - 1)$ information packets as explained in Section III-B. This structure efficiently retrieves the erased bits from the end points to the center of the protograph. However, if the coupling is too weak (namely N is small), the performance improvement via BP decoding would be limited and the SC-RACC would exhibit the error floor.

B. Triangle Distribution Channel

Figure 7 shows the decoding error rate (DER) of direct communication, conventional ANCC, and SC-RACC with $N = 4$ and 8 versus average bit erasure probability $\bar{\epsilon}$ of the triangle distribution channel where the decoding error is defined that the decoded codeword includes at least one bit erasure. In the following, the length of information packet K is 100 . The outage probabilities of direct communication and SC-RACC are also drawn in the figure.

As obvious from the figure, owing to the diversity gain, the slope of SC-RACC is steeper than that of direct communication and conventional ANCC meanwhile the direct

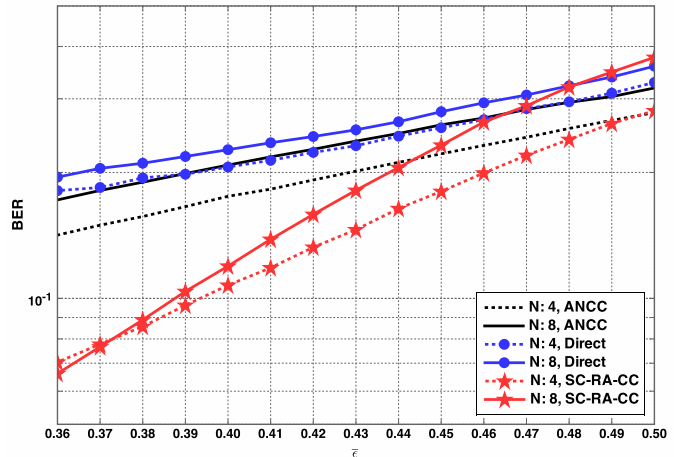


Fig. 8. BER versus average bit erasure probability $\bar{\epsilon}$ over triangle distributed channels.

communication and ANCC achieve the better performance at the high erasure probability region. In SC-RACC, the BP decoder retrieves the information from the end points to the center. The BP decoding, however, would stop when facing with burst erasures [16]. This phenomenon results in worse DER performance at the high erasure probability region. Also, as similar to the case with constant channel, the higher coding gain can be obtained by increasing N .

Finally, Fig. 8 shows the BER performance of direct communication, conventional ANCC, and SC-RACC with $N = 4$ and 8 over triangle distribution channels. Different from all the results shown above, the SC-RACC with small N provides the lower BER performance. When facing with the burst erasures, the BP decoding of SC-RACC causes more bit erasures in the codeword. When large N is utilized, the resulting protograph becomes sensitive to burst erasures. To overcome this issue, an attractive option is the use of multi-dimensional spatial coupling [16] or irregularly spatial coupling like Luby transform (LT) codes [17], which still remains as the future work.

VI. CONCLUSION

In this paper, we proposed SC-RACC and numerical results confirmed that SC-RACC can significantly improve the decoding performance even when the number of nodes and the length of information packets are limited.

ACKNOWLEDGMENT

This work was supported in part by JSPS KAKENHI Grant Number 24760295.

REFERENCES

- [1] I.F. Akyildiz, W. Su, Y. Sankarasubramaniam, and E. Cayirci, "A survey on sensor networks", *IEEE Commun. Mag.*, vol. 40, no. 8, pp. 102–114, Aug 2002.
- [2] L. Zheng and D.N.C. Tse, "Diversity and multiplexing: a fundamental tradeoff in multiple-antenna channels", *IEEE Trans. Inf. Theory.*, vol. 49, no. 5, pp. 1073–1096, May 2003.

- [3] V. Tarokh, H. Jafarkhani, and A.R. Calderbank, "Space-time block codes from orthogonal designs", *IEEE Trans. Inf. Theory.*, vol. 45, no. 5, pp. 1456–1467, Jul 1999.
- [4] C. Deqiang and J. Laneman, "Modulation and demodulation for cooperative diversity in wireless systems", *IEEE Trans. Wireless Commun.*, vol. 5, no. 7, pp. 1785–1794, July 2006.
- [5] T.E. Hunter and A. Nosratinia, "Diversity through coded cooperation", *IEEE Trans. Wireless Commun.*, vol. 5, no. 2, pp. 283–289, Feb 2006.
- [6] X. Bao and J. Li, "Adaptive network coded cooperation (ANCC) for wireless relay networks: matching code-on-graph with network-on-graph", *IEEE Trans. Wireless Commun.*, vol. 7, no. 2, pp. 574–583, February 2008.
- [7] R.G. Gallager, "Low-density parity-check codes", *IRE Trans. Inf. Theory.*, vol. 8, no. 1, pp. 21–28, January 1962.
- [8] J. Hou, P.H. Siegel, and L.B. Milstein, "Performance analysis and code optimization of low density parity-check codes on rayleigh fading channels", *IEEE J. Sel. Areas Commun.*, vol. 19, no. 5, pp. 924–934, May 2001.
- [9] D. Divsalar, H. Jin, and R. J. McEliece, "Coding theorems for 'turbo-like' codes", *Proc.36th Allerton Conf. on Commun. Control and Comput.*, pp. 201–210, September 1998.
- [10] C. Berrou, A Glavieux, and P. Thitimajshima, "Near Shannon limit error-correcting coding and decoding: Turbo-codes. 1", in *Proc. IEEE Int. Conf. Commun.*, Geneva, Switzerland, May 1993, vol. 2, pp. 1064–1070 vol.2.
- [11] A. Jimenez Felstrom and K.S. Zigangirov, "Time-varying periodic convolutional codes with low-density parity-check matrix", *IEEE Trans. Inf. Theory.*, vol. 45, no. 6, pp. 2181–2191, Sep 1999.
- [12] S. Johnson and G. Lechner, "Spatially coupled repeat-accumulate codes", *IEEE Commun. Lett.*, vol. 17, no. 2, pp. 373–376, February 2013.
- [13] J. Thorpe, "Low-density parity-check (LDPC) codes constructed from protographs", *JPL INP. Tech. Rep. 42-154*, Aug 2003.
- [14] F.R. Kschischang, B.J. Frey, and H.-A Loeliger, "Factor graphs and the sum-product algorithm", *IEEE Trans. Inf. Theory.*, vol. 47, no. 2, pp. 498–519, Feb 2001.
- [15] T.J. Richardson and R.L. Urbanke, "The capacity of low-density parity-check codes under message-passing decoding", *IEEE Trans. Inf. Theory.*, vol. 47, no. 2, pp. 599–618, Feb 2001.
- [16] R. Ohashi, K. Kasai, and K. Takeuchi, "Multi-dimensional spatially-coupled codes", in *Inf. Theory Proc. (ISIT)*, 2013 IEEE Int. Symposium on, July 2013, pp. 2448–2452.
- [17] M. Luby, "LT codes", in *Proc. 43rd Annual Symp. on Foundations of Computer Science (FOCS)*, 2002, pp. 271–280.